Molecular ionization energies and ground- and ionic-state properties using a non-Dyson electron propagator approach

A. B. Trofimov
Laboratory of Quantum Chemistry, Computer Center, Irkutsk State University, 664003 Irkutsk, Russian Federation

J. Schirmer[a)]
Theoretische Chemie, Physikalisch-Chemisches Institut, Universität Heidelberg, Im Neuenheimer Feld 229, D-69120 Heidelberg, Germany

(Received 13 July 2005; accepted 8 August 2005; published online 12 October 2005)

An earlier proposed propagator method for the treatment of molecular ionization is tested in first applications. The method referred to as the non-Dyson third-order algebraic-diagrammatic construction [nD-ADC(3)] approximation for the electron propagator represents a computationally promising alternative to the existing Dyson ADC(3) method. The advantage of the nD-ADC(3) scheme is that the $(N\pm1)$-electronic parts of the one-particle Green's function are decoupled from each other and the corresponding equations can be solved separately. For a test of the method the nD-ADC(3) results for the vertical ionization transitions in C_2H_4, CO, CS, F_2, H_2CO, H_2O, HF, N_2, and Ne are compared with available experimental and theoretical data including results of full configuration interaction (FCI) and coupled cluster computations. The mean error of the nD-ADC(3) ionization energies relative to the experimental and FCI results is about 0.2 eV. The nD-ADC(3) method, scaling as n^5 with the number of orbitals, requires the solution of a relatively simple Hermitian eigenvalue problem. The method renders access to ground-state properties such as dipole moments. Moreover, also one-electron properties of $(N\pm1)$ electron states can now be studied as a consequence of a specific intermediate-state representation (ISR) formulation of the nD-ADC approach. Corresponding second-order ISR equations are presented. © *2005 American Institute of Physics*. [DOI: 10.1063/1.2047550]

I. INTRODUCTION

Computational methods derived from the one-particle Green's function (or electron propagator) theory[1,2] have been firmly established in the field of quantum chemistry as standard tools for the calculation of ionization and electron attachment spectra.[3–12] The well-known advantages of these methods are the direct access to the properties of interest, a balanced treatment of the initial and final states, and the intrinsic size consistency.

Most of the electron propagator methods make use of the Dyson equation

$$\mathbf{G}(\omega) = \mathbf{G}^0(\omega) + \mathbf{G}^0(\omega)\mathbf{\Sigma}(\omega)\mathbf{G}(\omega) \tag{1}$$

which relates the exact one-particle Green's function $\mathbf{G}(\omega)$ to the so-called self-energy part $\mathbf{\Sigma}(\omega)$ and the free (zeroth-order) Green's function $\mathbf{G}^0(\omega)$.[1,2] A characteristic (and not always desirable) feature of the Dyson methods is that in these approaches, the $(N\pm1)$-particle parts of the one-particle Green's function ($\mathbf{G}^+$ and $\mathbf{G}^-$, respectively) are interconnected, and the resulting equations are defined with respect to configurational spaces comprising both $(N-1)$- and $(N+1)$-electron configurations.

Examples of Dyson propagator methods are approximation schemes derived within the algebraic-diagrammatic construction[13,14] (ADC), the equation-of-motion[15,16] (EOM) and the superoperator[17–19] approaches. Also the outer-valence Green's function[3,20] (OVGF) and the partial third-order[10] (P3) schemes are based on the perturbation expansions of the Dyson equation. Among these methods, a most successful approach is the third-order Dyson ADC scheme[14,21] [ADC(3)], which has been used in numerous applications (see, for example, Refs. 9, 22, and 23 and works cited therein).

Recently, a third-order ADC approximation for the electron propagator has been proposed, which does not employ the Dyson equation.[24] This non-Dyson (nD) ADC(3) scheme [nD-ADC(3)] has several important advantages over the previous Dyson ADC(3) scheme. The essential conceptual and computational simplification in the nD-ADC(3) scheme is achieved by the fact that the $(N-1)$- and $(N+1)$-electron problems are no longer coupled and can be treated separately. The nD-ADC(3) equations are thus defined with respect to much smaller configurational spaces. Moreover, distinct acceleration of convergence is expected in the iterative solution of the nD-ADC(3) secular equations, since the desired eigenvalues reside here at the low-energy margin of the spectrum, in contrast to the Dyson approach in which they are located in the middle of the spectrum. The nD-ADC(3) scheme scales as n^5 with respect to the number of orbitals n and can be considered as a useful alternative to the Dyson ADC(3) in large-scale calculations.

[a)]Electronic mail: h33@ix.urz.uni-heidelberg.de

The nD-ADC approach may be seen in a wider context comprising also the coupled-cluster (CC) methods for electron ionization based on the equation-of-motion[25] and linear-response[26] (LR) approaches. As demonstrated in Refs. 27–30, both the CC and ADC schemes can be viewed as specific intermediate-state representations (ISR) of the (shifted) Hamiltonian $\hat{H}-E_0$. The central computational step in these methods is the construction and diagonalization of a secular matrix, defined with respect to singly (S) doubly (D), triply (T), and higher excited $(N-1)$-electron configurations. The resulting eigenvalues give the (vertical) ionization energies, while the eigenvectors enter the evaluation of the corresponding spectroscopic amplitudes. The hierarchies of the ADC and CC approximations [ADC(n), $n=2,3,\ldots$, and CCSD, CCSDT, …] allow one to control the accuracy of the results and the computational cost in a systematic manner. All ADC and CC schemes are size consistent and can be used as black-box computational tools.

The EOM-CCSD method for the calculation of ionization potentials (IP) and the essentially equivalent symmetry-adapted cluster configuration interaction (SAC-CI) method[31] were frequently used in recent years (see, for example, Refs. 32 and 33, respectively). Recently, also the implementation and numerical test of the more accurate IP-EOM-CCSDT scheme was reported.[34] Some other schemes related to the nD-ADC approximation are the Fock-space CC (FSCC) method,[35] the consistent operator expansions of the electron propagator,[36] the CC Green's function approach[37–39] (CCGF), and the nh-$(n\pm1)p$ configuration interaction (CI) method.[40]

The objective of the present work is to test the performance of the nD-ADC(3) scheme, to establish an accuracy calibration, and to clarify certain theoretical aspects important for further implementations and applications of the method. The work aims at establishing nD-ADC(3) as an efficient and practical tool for large-scale computations. Since a calibration of any theoretical scheme can be made most rigorously against the results of full CI (FCI), we have performed nD-ADC(3) calculations for the same systems as in benchmark FCI calculations.[41–43] Additionally, we compare the nD-ADC(3) results to the experimental data for ionization energies of C_2H_4, CO, CS, F_2, H_2CO, H_2O, HF, N_2, and Ne,[44–47] which allows us to get better statistics for the performance of the nD-ADC(3) scheme. On the theoretical side, we compare our results with the results of the IP-EOM-CCSD and IP-EOM-CCSDT schemes.[34]

A less known application of the electron propagator theory is the evaluation of ground-state (GS) expectation values.[1] Since the present nD-ADC formalism allows for a direct access to the GS one-electron density matrix, computations of the one-electron properties can be easily implemented. The quality of the corresponding third-order approximation scheme is studied in the present paper for the example of ground-state dipole moments in CO, CS, H_2CO, H_2O, and HF. The results obtained here are compared with the available experimental data[48–52] and results of benchmark multireference CI calculations.

Finally, we discuss the possibility to evaluate expectation values and transition matrix elements for ionic $[(N\pm1)$-electronic$]$ states, which is enabled by the recent ISR formulation[53] of the nD-ADC approach. The second-order [ADC(2)] expressions required for ionic-state properties are presented.

II. THEORY

A. Non-Dyson ADC(3) method for electron propagator

The non-Dyson ADC approximation schemes[24] are obtained by applying the ADC procedure[13] separately to each of the $(N-1)$- and $(N+1)$-particle parts of the electron propagator $\mathbf{G}(\omega)$:

$$\mathbf{G}(\omega)=\mathbf{G}^{-}(\omega)+\mathbf{G}^{+}(\omega). \tag{2}$$

Obviously, the $\mathbf{G}^{-}(\omega)$ part is required for the ionization problem. In the original Dyson-type ADC approach the self-energy part $\mathbf{\Sigma}(\omega)$ of the Dyson equation [Eq. (1)] was subjected to the ADC treatment.[14]

The ADC technique[13,14] has proved to be a very useful tool for the derivation of the explicit ADC expressions. On the other hand, the recently proposed fully equivalent ISR approach offers a more direct and pedagogical way to the nD-ADC theory without the need to know the diagrammatic language.[27,28] Therefore, we will rely on the ISR formulation throughout this paper.

The nD-ADC method sets out from the general (nondiagonal) representation of $\mathbf{G}^{-}(\omega)$:

$$\mathbf{G}^{-}(\omega)^{t}=\mathbf{f}^{\dagger}(\omega-\mathbf{K}-\mathbf{C})^{-1}\mathbf{f}, \tag{2'}$$

where the "effective interaction" matrix $\mathbf{K}+\mathbf{C}$ is defined as a representation of the shifted Hamiltonian $\hat{H}-E_0$ in terms of the so-called "intermediate states" $|\tilde{\Psi}_J^{N-1}\rangle$ (Refs. 27 and 28),

$$(\mathbf{K}+\mathbf{C})_{IJ}=-\langle\tilde{\Psi}_I^{N-1}|\hat{H}-E_0|\tilde{\Psi}_J^{N-1}\rangle \tag{3}$$

and the "effective transition moments" are defined as

$$f_{I,q}=\langle\tilde{\Psi}_I^{N-1}|c_q|\Psi_0^N\rangle. \tag{4}$$

In Eqs. (2)–(4) $|\Psi_0^N\rangle$ and E_0 denote the exact N-electron ground state and the ground-state energy, respectively, and $\hat{H}$ is the Hamiltonian of the system; $c_q(c_q^{\dagger})$ denote destruction (creation) operators associated with Hartree-Fock (HF) orbitals $|\varphi_q\rangle$. The intermediate states $|\tilde{\Psi}_J^{N-1}\rangle$ are generated by a specific orthonormalization procedure from the correlated $(N-1)$-electron states

$$|\Psi_J^{\#}\rangle=\hat{C}_J|\Psi_0^N\rangle, \tag{5}$$

where $\hat{C}_J$ denote operators generating one-hole (1h), one-particle–two-hole $(1p\text{-}2h),\ldots$, configurations:

$$\{\hat{C}_J\}=\{c_k, c_a^{\dagger}c_kc_l, c_a^{\dagger}c_b^{\dagger}c_kc_lc_m, \ldots;\ a<b<\ldots;k<l<m<\ldots\}. \tag{6}$$

Here and in the following the subscripts $i,j,k,\ldots$, and $a,b,c,\ldots$, refer to occupied and unoccupied orbitals, respectively. The subscripts $p,q,r,\ldots$, label both occupied and unoccupied orbitals.

The intermediate states $|\tilde{\Psi}_J^{N-1}\rangle$ are related to the exact

states $|\Psi_m^{N-1}\rangle$ *via* a transformation:

$$|\Psi_m^{N-1}\rangle = \sum_J Y_{Jm} |\tilde{\Psi}_J^{N-1}\rangle. \tag{7}$$

In the basis of exact states $|\Psi_m^{N-1}\rangle$ Eq. (2) takes on the diagonal form, also known as spectral representation, in which the physical contents of the electron propagator becomes explicit:

$$\mathbf{G}^-(\omega)^t = \mathbf{x}^\dagger(\omega - \Omega)^{-1}\mathbf{x}. \tag{8}$$

Here Ω denotes the diagonal matrix of (negative) vertical ionization energies,

$$\Omega_{mm} = -(E_m^{N-1} - E_0^N) \tag{9}$$

and the vectors $\mathbf{x}$ denote spectroscopic amplitudes, related to spectral intensities,

$$x_{mq} = \langle \Psi_m^{N-1} | c_q | \Psi_0^N \rangle. \tag{10}$$

The simplest form of the (relative) photoelectron spectral intensities P_m can be evaluated according to

$$P_m = \sum_q |x_{m,q}|^2.$$

The transformation of $\mathbf{G}^-(\omega)$ from the ADC representation [Eq. (2′)] to the spectral representation [Eq. (8)] is equivalent to the solution of the Hermitian eigenvalue problem for the matrix $\mathbf{K}+\mathbf{C}$,

$$(\mathbf{K}+\mathbf{C})\mathbf{Y} = \mathbf{Y}\boldsymbol{\Omega}, \quad \mathbf{Y}^\dagger\mathbf{Y} = 1, \tag{11}$$

where the $\mathbf{Y}$ denotes the matrix of eigenvectors. The eigenvectors of $\mathbf{Y}$ form the transformation matrix relating the intermediate states and exact states,

$$Y_{Jm} = \langle \tilde{\Psi}_J^{N-1} | \Psi_m^{N-1} \rangle. \tag{12}$$

The spectroscopic amplitudes $\mathbf{x}$ can be obtained from the effective transition moments $\mathbf{f}$ according to

$$\mathbf{x} = \mathbf{Y}^\dagger\mathbf{f}. \tag{13}$$

The nD-ADC approximation schemes for $\mathbf{G}^-(\omega)$ [Eq. (2′)] are obtained by truncating the expansion manifold [Eq. (7)] and by employing consistent perturbation expansions for the matrix elements of the effective interaction and transition moments:

$$\mathbf{K}+\mathbf{C} = \mathbf{K}^{(0)} + \mathbf{C}^{(1)} + \mathbf{C}^{(2)} + \cdots, \tag{14a}$$

$$\mathbf{f} = \mathbf{f}^{(0)} + \mathbf{f}^{(1)} + \mathbf{f}^{(2)} + \cdots. \tag{14b}$$

The explicit expressions for the elements of $\mathbf{K}+\mathbf{C}$ and $\mathbf{f}$ can be derived using the Rayleigh-Schrödinger perturbation theory (RSPT) for $|\Psi_0^N\rangle$ and E_0 (Ref. 27), or by the ADC procedure operating with the diagrammatic perturbation expansion for $\mathbf{G}^-(\omega)$.[24]

In Fig. 1 we show schematically the block structure of the $\mathbf{K}+\mathbf{C}$ and $\mathbf{f}$ matrices and the required orders of perturbation theory in the respective blocks for various nD-ADC schemes. At second order, the $\mathbf{K}+\mathbf{C}$ matrix comprises the zeroth- and second-order $1h/1h$ block, the first-order $1h/1p$-$2h$ block, and the zeroth-order $1p$-$2h/1p$-$2h$ block. At the ADC(3) level, the $\mathbf{K}+\mathbf{C}$ matrix is extended by third-, second- and first-order contributions to the $1h/1h$, $1h/1p$-$2h$, and $1p$-$2h/1p$-$2h$ blocks, respectively. The extended second-order scheme [nD-ADC(2)-E] improves the strict nD-ADC(2) scheme by taking into account the first-order matrix elements of the $1p$-$2h/1p$-$2h$ block.

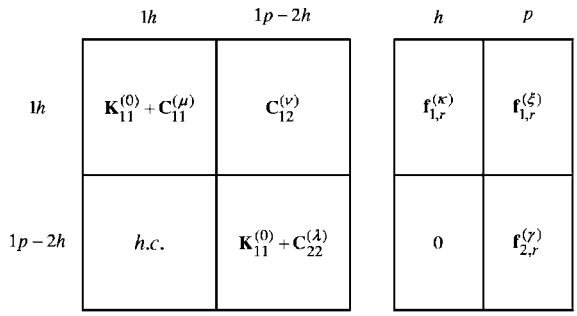

Scheme	μ	ν	λ	κ	ξ	γ
ADC(3)	2, 3	1, 2	1	0, 2, 3	2, 3	1, 2
ADC(2)-E	2	1	1	0, 2	2	1
ADC(2)	2	1	–	0, 2	2	1

(c)

FIG. 1. Block structure of the secular matrix $\mathbf{K}+\mathbf{C}$ (a) and of the matrix of transition amplitudes $\mathbf{f}$ (b); order of perturbation-theoretical expansions for the matrix elements at the nD-ADC(3) and lower nD-ADC levels (c).

The explicit nD-ADC expressions through third order have been given in Appendix A of Ref. 24. In the present work an equivalent (more symmetric) form of the third-order contributions to the $1h$ diagonal blocks of $\mathbf{K}+\mathbf{C}$ and $\mathbf{f}$ matrices has been used, which is better adapted to the computer implementation. The corresponding expressions are collected and discussed in Appendix A.

The ADC method combines the eigenvalue problem of a Hermitian secular matrix and perturbation theory for the secular matrix elements. With respect to convergence, the (finite) perturbation expansions used for the matrix elements behave as the ground-state RSPT series. At the nD-ADC(3) level, the $1h$ and $1p$-$2h$ ionization transitions are treated consistently through third and first orders, respectively. In general, the truncation error (for $1h$ configurations) due to restricting the explicit nD-ADC configuration space to the μ lowest configuration classes $1h$, $1p$-$2h$, …, $(\mu$-$1)p$-μh is of the order 2μ (*compactness* property). This is a consequence of the "canonical" order relations[28] holding for the ADC secular matrices. Another basic property of ADC is the *separability* of the secular matrices.[54] This property guarantees size-intensive ionization energies and transition amplitudes, which is a crucial requirement for the application to large systems.

B. Improved treatment of static self-energy and one-particle densities

One of the issues to be discussed here is the choice of an appropriate approximation for the so-called static self-energy $\boldsymbol{\Sigma}(\infty)$, which contributes to the matrix elements $C_{kk'}^{(3)}$ and $f_{ka}^{(3)}$:

$$C^{(3)}_{kk'} = C^{(A)}_{kk'} + C^{(B)}_{kk'} + C^{(C)}_{kk'} + C^{(D)}_{kk'} + \Sigma^{(3)}_{k'k}(\infty), \tag{15}$$

$$f^{(3)}_{ka} = \frac{1}{\varepsilon_k - \varepsilon_a}(\Sigma^{(3)}_{ak}(\infty) + M^{(3)+}_{ak}(\varepsilon_k) + M^{(3)-}_{ak}(\varepsilon_a)). \tag{16}$$

Here $M^{(3)\pm}_{ak}(\omega)$ is the third-order dynamic self-energy contributions,[8] $C^{(A-D)}_{kk'}$ are the contributions specified in Ref. 24, and ε_q denotes HF orbital energies. As demonstrated in Refs. 21, 30, and 55, a perturbative treatment of $\mathbf{\Sigma}(\infty)$ is not always satisfactory, and one has to go beyond the strict third-order expressions in order to achieve a systematical improvement. A general procedure for the evaluation of $\mathbf{\Sigma}(\infty)$ through fourth order of the perturbation theory including infinite partial summations of higher-order terms, referred to as the Dyson-expansion method (DEM), was developed and used in combination with the Dyson ADC(3) scheme.[21] The DEM for $\mathbf{\Sigma}(\infty)$ can readily be adopted for the nD-ADC(3) scheme. A disadvantage of the DEM, however, is that one has to deal also with the $1h$-$2p$ states of $N+1$ electrons. Clearly in the context of the nD-ADC method it would be more appealing to have an approximation for $\mathbf{\Sigma}(\infty)$ circumventing the necessity to take $(N+1)$-electron states into account. In the present work we study several such schemes for $\mathbf{\Sigma}(\infty)$ with respect to accuracy, convergence properties, and computational cost.

The matrix elements of the static self-energy can be written as[3]

$$\Sigma_{pq}(\infty) = \sum_{r,s} V_{pr[qs]}\rho^c_{sr}, \tag{17}$$

where

$$\rho^c_{sr} = \langle\Psi_0|c^\dagger_r c_s|\Psi_0\rangle - \langle\Phi_0|c^\dagger_r c_s|\Phi_0\rangle \tag{18}$$

are the matrix elements of the correlation density, that is, the difference $\boldsymbol{\rho}^c = \boldsymbol{\rho} - \boldsymbol{\rho}^{(0)}$ between the exact GS one-particle density matrix and the HF density matrix, $\rho^{(0)}_{rs} = n_r\delta_{rs}$, and $V_{pr[qs]} = V_{prqs} - V_{prsq}$ denote antisymmetrized Coulomb integrals in the "1212" notation. As the zeroth- and first-order contributions to $\boldsymbol{\rho}^c$ vanish, the static self-energy matrix elements arise for the first time in third order being, however, not well approximated at that level in general. It is therefore advisable to replace the strict third-order expressions for $\mathbf{\Sigma}(\infty)$ in Eqs. (15) and (16) by improved results. A fourth-order approximation for $\mathbf{\Sigma}(\infty)$ can be obtained by substituting a third-order expression for $\boldsymbol{\rho}^c$ in Eq. (17). The latter is readily available at the nD-ADC(3) level because of the relation[24]

$$\boldsymbol{\rho} = \mathbf{f}^\dagger\mathbf{f} \tag{19}$$

which follows from Eqs. (4) and (18). Because the p-h matrix elements of $\mathbf{f}^{(3)}$ depend on $\mathbf{\Sigma}(\infty)$, Eqs. (16)–(19) represent a set of linear inhomogeneous equations for the matrix elements of $\mathbf{\Sigma}(\infty)$. They can be solved by an iterative procedure. This procedure, referred to as $\Sigma(4+)$ in the following, can be viewed as a simplification of the DEM scheme: the inhomogeneities, b_{pq}, on the right-hand side of Eq. (25a) of Ref. 21 are evaluated through fourth order of the perturbation theory. The corresponding perturbational expressions can readily be derived using the explicit third-order expansions for the matrix elements of $\boldsymbol{\rho}^c$ as given in Eqs. (A33)–(A36) of Ref. 24. Here, for consistency, the perturbation expansions for $\boldsymbol{\rho}^c$ (or b_{pq}) should be truncated strictly at the third (fourth) order. Without such a restriction, the evaluation of $\boldsymbol{\rho}$ according to Eq. (19) at the nD-ADC(3) would lead to contributions up to sixth order of perturbation theory (PT).

For further reference we introduce here notations for the $\mathbf{\Sigma}(\infty)$-approximation schemes: $\Sigma(3)$, $\Sigma(4)$, $\Sigma(4+)$, and Σ(DEM) denote, respectively, the strict third-order, strict third- plus-fourth-order, improved fourth-order [according to Eqs. (16)–(19)], and the DEM (Ref. 21) schemes. Since the DEM was established as a standard procedure, the notation nD-ADC(3) will imply the DEM approximation unless otherwise stated.

C. Ground-state one-electron properties

The easy access to the ground-state one-particle density matrix in the nD-ADC method via Eq. (19) allows one to compute in a standard manner the ground-state expectation values $\langle\hat{A}\rangle$ of a one-particle operator

$$\hat{A} = \sum_{r,s} A_{rs}c^\dagger_r c_s \tag{20}$$

according to

$$\langle\hat{A}\rangle = \mathrm{Tr}(\mathbf{A}\boldsymbol{\rho}). \tag{21}$$

Here $\mathbf{A}$ is the matrix of one-particle elements $A_{rs} = \langle\varphi_r|\hat{a}|\varphi_s\rangle$. As an example, we will consider the dipole moment operator $\hat{D} = \Sigma_\mu \hat{D}_\mu$ (where index μ runs over x-, y- and z-Cartesian components) in Sec. III.

D. One-electron properties of molecules in ionic states

The ISR formalism[27,28] opens new possibilities unavailable in the conventional propagator approach. In particular, the evaluation of one-electron properties of the final ionic states becomes possible.[53] Using Eq. (7), transition matrix elements D_{mn} of arbitrary one-particle operator $\hat{D}$ can be written as

$$\begin{aligned} D_{mn} &= \langle\Psi^{N\pm1}_m|\hat{D}|\Psi^{N\pm1}_n\rangle \\ &= \sum_{I,J} Y^*_{mI}\langle\tilde{\Psi}^{N\pm1}_I|\hat{D}|\tilde{\Psi}^{N\pm1}_J\rangle Y_{nJ} = \mathbf{Y}^\dagger_m\tilde{\mathbf{D}}\mathbf{Y}_n, \end{aligned} \tag{22}$$

where the matrix $\tilde{\mathbf{D}}$ with elements $\tilde{D}_{IJ} = \langle\tilde{\Psi}^{N\pm1}_I|\hat{D}|\tilde{\Psi}^{N\pm1}_J\rangle$ is the intermediate-state representation of the operator $\hat{D}$ and $\mathbf{Y}_n$ are the eigenvectors of Eq. (11).

The matrix $\tilde{\mathbf{D}}$ has a similar block and order structure as the $\mathbf{K}+\mathbf{C}$ matrix and possesses all ADC/ISR properties discussed in Sec. II A. The explicit expressions for the matrix elements $\tilde{D}_{IJ}$ can be obtained using perturbation theory. In Ref. 53 the $\tilde{D}_{IJ}$ expressions for the excitation problem (N-electron case) have been derived through second order of PT. Here we present the corresponding second-order ISR ex-

TABLE I. Characteristics of nD-ADC and CC methods (explicit configuration space, perturbation-theoretical consistency for ionization energies (Ω), and ground-state (E_0) energies scaling).

Method	Configuration space	Ω		E_0	Scaling[a]
		$1h$	$2h$-$1p$		
ADC(2)	$1h$, $2h$-$1p$	2	0	2	n^4
ADC(2)-E	$1h$, $2h$-$1p$	2	1	2	n^5
CCSD	$1h$, $2h$-$1p$	2	1	3	n^6
ADC(3)	$1h$, $2h$-$1p$	3	1	3	n^5
CCSDT	$1h$, $2h$-$1p$, $3h$-$2p$	3	2	4	n^8

[a]For the CC schemes the scaling refers to the ground-state calculations, which is the computationally most expensive step (see text for details).

pressions for the ionic ($N\pm1$) electron states. The derivation follows closely the procedure described in Ref. 53. The results are collected in Appendix B.

E. Comparison with coupled-cluster methods

As the nD-ADC schemes, the CC approach to electronic ionization[25,26,31] can be viewed as a specific intermediate-state representations of the shifted Hamiltonian $\hat{H}-E_0$. In the CC case two different sets of intermediate states are employed: the $(N-1)$-electronic excited states of the form $|\hat{\Psi}_J^{N-1}\rangle=\hat{C}_J e^{\hat{T}}|\Phi_0\rangle$ and the corresponding biorthogonal states $\langle\check{\Psi}_I^{N-1}|=\langle\Phi_0|\hat{C}_I^{\dagger}e^{-\hat{T}}$. Here $\hat{C}_J$ are operators defined by Eq. (6) and $e^{\hat{T}}|\Phi_0\rangle$ is the standard CC parameterization of the N-electronic ground-state $|\Psi_0^N\rangle$ using the cluster operator of the form $\hat{T}=\hat{T}_1+\hat{T}_2+\cdots$. The secular matrix of the resulting biorthogonal coupled-cluster representation,

$$M_{IJ}=\langle\check{\Psi}_I|\hat{H}-E_0|\hat{\Psi}_J\rangle, \tag{23}$$

is non-Hermitian giving rise to a right- and left- hand eigenvalue problem,

$$\mathbf{MX}=\mathbf{X\Omega}, \quad \mathbf{Y}^{\dagger}\mathbf{M}=\mathbf{\Omega Y}^{\dagger}, \quad \mathbf{Y}^{\dagger}\mathbf{X}=1. \tag{24}$$

The hierarchy of CC approximation schemes is obtained by extending the $(N-1)$-electronic configuration space to S, SD, SDT, …, configuration classes (here also denoted as $1h$, $1p$-$2h$, $2p$-$3h$,…, respectively) and by introducing approximations to the CC amplitudes (for the N-electronic ground state) and the secular matrix elements.

The CCSD approximation employs an explicit configuration space of $1h$ and $1p$-$2h$ configurations and the SD cluster amplitudes (Table I). This yields a consistent second-order treatment of single-hole states and a first-order treatment of $1p$-$2h$ states. The numerical cost of CCSD involving the construction and solution of Eq. (24) is proportional to n^5. On the other hand, the solution of the CCSD ground-state equations for the cluster amplitudes scales as n^6, so that the overall cost of the method is proportional to n^6. A comparable theoretical description of the $1h$ and $1p$-$2h$ states is yielded by the nD-ADC(2)-E scheme for which the computational cost is proportional to n^5. The strict second-order nD-ADC(2) scheme, treating the $1p$-$2h$ states through zeroth order, scales even more favorably as n^4.

As follows from the theoretical analysis in Ref. 28, the CC configuration space must comprise the $2p$-$3h$ configurations in order to have third-order consistency for single-hole states. This is the case in the CCSDT method. The method scales as n^7 in the treatment of Eq. (24) and as n^8 in the solution of the ground-state CCSDT problem. The resulting CCSDT computational costs are therefore proportional to n^8. The third-order consistency of the CCSDT model (for single-hole states) is shared by the less expensive nD-ADC(3) method, which scales only as n^5. As a consequence of the compactness property,[28] the configuration space of the nD-ADC(3) scheme does not include the $2p$-$3h$ configurations. The explicit consideration of the $2p$-$3h$ configurations in the CCSDT allows for a better, namely, consistent second-order treatment of the $1p$-$2h$ states, which at the nD-ADC(3) level are treated consistently through first order only. In view of the importance of the admixture of $1p$-$2h$ configurations in the single-hole states, the CCSDT results will, in general, be more accurate than those of the nD-ADC(3) treatment.

III. COMPUTATIONS

The present prototypical nD-ADC(3) implementation follows the conventional strategy in which one first computes and stores the nonvanishing secular matrix elements and then, in a second step, performs the (iterative) diagonalization. This procedure has still an unfavorable scaling, but it allows for a straightforward and utmost error-free implementation of the method, which was our main objective at the present stage. The development of a code optimized with respect to computational efficiency and exploiting the full n^5 scaling potential of the nD-ADC(3) method will be the next logical step. Here, the key point is a direct diagonalization procedure in which (parts of) the secular matrix are recomputed as needed in performing the matrix-vector products,

$$\bar{Y}_{In}=\sum_J (K+C)_{IJ}Y_{Jn}, \tag{25}$$

required in the iterative solution of Eq. (11). As one can easily check, all such products in the nD-ADC(3) scheme can be broken down to utmost n^5 steps by forming appropriate intermediates (see Ref. 30 for a more detailed discussion in the case of an ADC secular matrix and Ref. 56 for similar techniques in the context of CC methods). The scaling properties of the nD-ADC schemes in Table I refer to such a direct diagonalization.

The explicit expressions for the nD-ADC(3) secular matrix elements in Ref. 24 have been given in spin-orbital form. For program implementation, the spin-free working equations for the final-state spin values $S=1/2$ and $3/2$ have been generated. Simultaneously, summations over spin variables have been performed. More details of the procedure used at this step can be found in Ref. 30. The present nD-ADC(3) code was interfaced to the GAMESS (US) (Ref. 57) and MOLCAS (Refs. 58 and 59) program packages.

For comparison with the experimental data, the nD-ADC calculations were performed for the following systems: C_2H_4, CO, CS, F_2, H_2CO, H_2O, HF, N_2, and Ne. Experimental equilibrium ground-state geometrical parameters were

used in the calculations. The CO, CS, F_2, HF, and N_2 internuclear distances (1.128, 1.535, 1.412, 0.917, and 1.098 Å, respectively) were taken from Ref. 60. Geometries for C_2H_4 ($R_{CC}=1.33$ Å, $R_{CH}=1.08$ Å, $\angle HCC=117.4°$), H_2CO ($R_{CO}=1.21$ Å, $R_{CH}=1.12$ Å, $\angle HCH=116.5°$), and H_2O ($R_{OH}=0.96$ Å, $\angle HOH=104.5°$) were taken from Refs. 61–63, respectively. The aug-cc-pVTZ basis set[64] was used for Ne. For the other examples the aug-cc-pVDZ basis set was employed (exceptions are C_2H_4 and H_2CO molecules, where the cc-pVDZ basis was used for the hydrogen atoms).[64] Throughout, the Cartesian representation of the *d*- and *f*-basis functions was used.

In order to study the accuracy of the nD-ADC ionization energies with respect to FCI data, calculations were performed for H_2O, CH_2, and F^- for which FCI results are available (Refs. 41–43, respectively). The same set of ground-state equilibrium geometrical parameters and basis sets as in Refs. 41–43 was used in these calculations.

Comparison of the nD-ADC and IP-EOM-CC results was done for the CO, F_2, and N_2 molecules. For these molecules IP-EOM-CC calculations have been reported in Ref. 34. The same set of the ground-state equilibrium geometries and basis sets was employed in our nD-ADC calculations.

For a test of the nD-ADC(3) results for ground-state one-electron properties, a series of molecules (CO, CS, H_2CO, H_2O, and HF) possessing dipole moments was considered. The dipole moment calculations were performed using the same basis sets and geometrical parameters as in the corresponding computations for the comparison with experiment. To generate theoretical benchmarks for the GS dipole moments, we have carried out multireference CI (MRCI) calculations including all singly and doubly excited configurations. In the MRCI calculations the C1*s*, O1*s*, F1*s*, S1*s*, S2*s*, and S2*p* orbitals were kept frozen; the weight of the reference space was at least 0.9. The MRCI calculations were performed using the direct CI program[65] from the GAMESS-UK package.[66]

Benchmark curves for the dependence of the diagonal components of the static self-energy on the internuclear distance in CO were generated using the single, double, triple, and quadruple configuration interactions (SDTQ-CI) method as implemented in the MOLCAS package.[58] Here the $(9s5p)/4s2p$ DZ basis set of Dunning and co-worker[67] was used. An additional code for the evaluation of the self-energy components from the SDTQ-CI one-electron densities according to Eq. (17) was employed.[68] In these calculations, the C1*s* and O1*s* orbitals were kept frozen. Calculations were performed for nine points in the range of the internuclear distances from 0.928 to 1.328 Å with the step of 0.05 Å.

For the conversion of units the factor 1 hartree =27.211 606 eV was used.

IV. RESULTS AND DISCUSSION

A. nD-ADC(3) ionization energies

1. Comparison with experimental data

In Table II we compare the HF (Koopmans), nD-ADC(2), and nD-ADC(3) results for the lowest vertical ionization transitions in C_2H_4, CO, CS, F_2, H_2CO, H_2O, HF, N_2, and Ne with experimental data.[44–47] The results of the original Dyson ADC(3) scheme[14,21,69] are also shown for comparison. Typically, the results of the Dyson and non-Dyson ADC(3) versions differ by less than 0.1 eV. Therefore, the accuracy calibration given here for the nD-ADC(3) method applies also to the Dyson ADC(3) version, and we may drop the distinction between the two variants whenever unessential. For the evaluation of mean and maximum errors we select 25 transitions with $P>0.65$, that is, ionic states of dominant single-hole character. Here a remark concerning the comparison of theoretical and experimental ionization potentials is appropriate. As is well known, the vertical ionization energies obtained from the electronic computations cannot directly be measured. Usually, the centroid of an experimental band is assigned to the corresponding vertical IP. But this is an approximation, and the centroids may deviate from the "true" vertical IP by up to 0.3 eV in unfavorable cases. [The true vertical IP can be extracted from experiment only by an analysis of the vibrational structure based on a suitable (theoretical) model of the vibrational excitation.] For the mean deviation between theory and experiment the errors in the experimental vertical IPs will average out to a certain extent so that this quantity is significant. The maximal deviations, on the other hand, must be relativized because here also the experimental uncertainties will play a role.

The second-order [nD-ADC(2)] method provides some improvement with respect to the HF level. In particular, it restores the correct order of energy levels, when they are incorrectly predicted at the HF level (e.g., the $7\sigma^{-1}$ and $2\pi^{-1}$ transitions in CS molecule). However, the average error here, 0.9 eV, is still quite large. The nD-ADC(2) scheme does not take into account the mutual interaction of $1p$-$2h$ states (Fig. 1). Thus, ionic states with dominant $1p$-$2h$ character cannot be recovered (e.g., satellites accompanying the $1b_{3u}^{-1}$ and $2b_u^{-1}$ transitions in C_2H_4, the $6\sigma^{-1}$ transition in CS, and the $1b_2^{-1}$ transition in H_2CO).

The results are distinctly improved at the nD-ADC(3) level, where the average error reduces to 0.23 eV and the maximal error is 0.65 eV. The maximal deviation arises for the $1b_2^{-1}$ transition of H_2O, other large deviations are seen for the 4σ ionization in CO, and the $1b_{2u}$ and $3a_g$ ionization in C_2H_4. It should be noted that the generally accepted experimental values listed in Table II correspond partly to the maxima of the respective bands rather than to the centroids. As an inspection of the experimental spectra indicates, the centroids would clearly lie at higher energy in the case of H_2O and CO and at lower energy in C_2H_4. This means that the actual discrepancies between the ADC(3) results and the experimental vertical ionization energies should be less dramatic than those displayed in Table II. In the case of the $1b_2^{-1}$ ionization of H_2O this expectation is supported by the excellent agreement between the nD-ADC(3) and the FCI result (see below).

The accuracy of the nD-ADC(3) with respect to transitions with increased $1p$-$2h$ character is less satisfactory.

TABLE II. Vertical ionization energies Ω(eV) and spectroscopic factors P obtained using HF (Koopmans), nD-ADC(2), nD-ADC(3), and Dyson ADC(3) methods. The last two lines give the mean absolute error $\bar{\Delta}_{abs}$ and the maximum absolute error Δ_{max} relative to the experimental data (eV).

System, $1h$ configuration	HF	nD-ADC(2)		nD-ADC(3)		Dyson ADC(3)		Expt.[a]
	Ω	Ω	P	Ω	P	Ω	P	Ω
C_2H_4								
$1b_{2u}$	10.25	10.15	0.90	10.46	0.91	10.52	0.91	10.95
$1b_{2g}$	14.03	12.79	0.91	13.19	0.91	13.26	0.91	12.95
$3a_g$	15.46	13.79	0.89	14.36	0.91	14.43	0.91	14.88
$1b_{3u}$	17.96	16.13	0.87	16.49	0.79	16.56	0.79	16.34
				18.12	0.06	18.12	0.06	17.8
$2b_{1u}$	21.32	18.96	0.86	19.00	0.64	19.06	0.62	19.40
				20.02	0.16	20.03	0.17	20.45
CO								
5σ	15.08	13.78	0.91	13.80	0.89	13.94	0.89	14.01
1π	17.43	16.23	0.89	16.88	0.90	16.98	0.90	16.91
4σ	21.99	18.30	0.85	20.10	0.79	20.19	0.78	19.72
CS								
7σ	12.85	11.00	0.86	11.33	0.85	11.51	0.85	11.4
2π	12.64	12.84	0.91	12.66	0.90	12.74	0.90	13.0
6σ	18.89	16.89	0.85	15.51	0.19	15.54	0.18	16.1
				17.94	0.68	18.02	0.69	18.05
F_2								
$1\pi_g$	18.19	13.88	0.87	15.87	0.90	15.97	0.90	15.83
$1\pi_u$	22.13	17.03	0.84	19.11	0.81	19.23	0.81	18.8
$3\sigma_g$	20.59	20.24	0.89	21.01	0.88	21.13	0.88	21.1
H_2CO								
$2b_2$	11.99	9.33	0.87	10.87	0.91	10.97	0.91	10.88
$1b_1$	14.53	13.71	0.88	14.30	0.88	14.43	0.88	14.5
$5a_1$	17.48	14.45	0.86	16.20	0.90	16.28	0.90	16.0
$1b_2$	19.09	17.00	0.88	17.32	0.65	17.39	0.62	16.6
				18.37	0.21	18.39	0.24	
H_2O								
$1b_1$	13.85	11.22	0.88	12.78	0.92	12.86	0.93	12.62
$3a_1$	15.91	13.53	0.89	15.08	0.93	15.15	0.93	14.74
$1b_2$	19.52	17.95	0.90	19.16	0.93	19.21	0.93	18.51
HF								
1π	17.69	14.39	0.89	16.41	0.93	16.48	0.93	16.05
3σ	20.97	18.67	0.90	20.30	0.94	20.36	0.94	20.0
N_2								
$3\sigma_g$	17.25	14.79	0.88	15.60	0.91	15.72	0.91	15.60
$1\pi_u$	16.74	16.99	0.91	16.77	0.92	16.85	0.92	16.98
$2\sigma_u$	21.25	17.99	0.85	18.93	0.82	19.06	0.81	18.78
Ne								
$2p$	23.15	20.07	0.91	21.84	0.94	21.88	0.94	21.60
$\bar{\Delta}_{abs}$[b]	1.39	0.91		0.23		0.26		
Δ_{max}[b]	3.33	1.95		0.65		0.70		

[a]Experimental vertical ionization energies for C_2H_4, CS, and Ne are from Refs. 44–46, respectively; the remaining data are from Ref. 47.
[b]Only transitions with $P>0.65$ are taken into account.

Since the $1p$-$2h$ configurations are treated consistently through first order only, the error increases when the role of such configurations in the final state grows. Examples are the $6\sigma^{-1}$ transition in CS and the $1b_2^{-1}$ transition in H_2CO for which an error of 0.6–0.7 eV is found.

2. Comparison with FCI results

Of course, the ultimate accuracy test for a computational method is the comparison with FCI. Unfortunately, only few FCI calculations of ionic states are available in the literature.

TABLE III. Comparison of vertical ionization energies (eV) obtained using HF (Koopmans), nD-ADC(2), and nD-ADC(3) schemes with the results of FCI. $\bar{\Delta}_{abs}$ and Δ_{max} are the mean and the maximum absolute errors, respectively, relative to FCI (eV).

System, $1h$ configuration	HF	nD-ADC(2)	nD-ADC(3)	FCI[a]
H_2O				
$1b_1$	13.32	10.83	12.06	11.84
$3a_1$	14.74	12.92	14.01	13.85
$1b_2$	18.51	17.94	18.65	18.60
$\bar{\Delta}_{abs}$	0.82	0.87	0.14	
Δ_{max}	1.48	1.01	0.22	
CH_2				
$3a_1$	10.66	9.86	9.95	10.26
$1b_2$	15.29	14.71	14.80	14.85
$2a_1$	24.18	22.71	22.22	22.14
$\bar{\Delta}_{abs}$	0.96	0.37	0.15	
Δ_{max}	2.04	0.57	0.31	
F^-				
^2P[b]	4.82	0.71	3.49	2.90
^2P[c]	4.82	0.80	3.52	3.03
^2P[d]	4.83	0.98	3.64	3.04
$\bar{\Delta}_{abs}$	1.83	2.16	0.56	
Δ_{max}	1.92	2.23	0.60	

[a]The FCI results for H_2O, CH_2, and F^- are from Refs. 41–43, respectively.
[b][$4s3p1d$] basis Ref. 43.
[c][$4s3p2d$] basis Ref. 43.
[d][$5s4p2d$] basis Ref. 43.

FCI results for H_2O,[41] CH_2,[42] and F^- (Ref. 43) are compared in Table III with nD-ADC results obtained using the same basis sets and geometries.

Whereas the H_2O molecule is a standard example, CH_2 and F^- are difficult cases. The CH_2 molecule is of quasi-open-shell type, lacking a distinct energy gap between occupied and virtual orbitals. Its ground state cannot be adequately treated in terms of RSPT, so that also the applicability of the ADC methods is affected. Also, in our calculations, we had to use the closed-shell $1\,^1A_1$ state as the reference state, since the true ground state of CH_2 ($1\,^3B_1$) has open-shell configuration. Also F^- is a difficult task for the ADC method which is reflected by the large energy oscillations between the HF, ADC(2), and ADC(3) results.

As seen in Table III, the performance of the nD-ADC(3) method for H_2O is very good. The mean and maximum error is 0.14 and 0.22 eV, respectively. The ionization energy of 18.65 eV obtained for the $1b_2^{-1}$ transition, which differed so distinctly from the experimental IP in Table II, is now in excellent agreement with the FCI value of 18.60 eV. Despite the complex electronic structure of the CH_2 system, the nD-ADC(3) performs here nearly as well as in H_2O (the mean and maximum error is 0.15 and 0.31 eV, respectively). Already the nD-ADC(2) results for CH_2 are not too bad (the mean and maximum error is 0.37 and 0.57 eV, respectively).

In the case of F^-, following Ref. 43 we compare results for the ^2P ionization potential obtained using three basis sets of improving quality: [$4s3p1d$], [$4s3p2d$], and [$5s4p2d$]. The discrepancies between the ADC(3) and FCI results are in the range of 0.6 eV, quite independent of the basis sets. The distinct oscillatory convergence pattern of the HF, ADC(2), and ADC(3) results suggests that a more precise IP can only be expected at the next higher level of theory, that is, ADC(4).

TABLE IV. Comparison of vertical ionization energies (eV) obtained using the nD-ADC(3) scheme with IP-EOM-CC results. Equilibrium ground-state geometrical parameters and basis sets from Ref. 34. The last two lines give the mean absolute error $\bar{\Delta}_{abs}$ and the maximum absolute error Δ_{max} relative to the experimental data (eV).

System, $1h$ configuration	HF	nD-ADC(3)	CCSD[a]	CCSDT[a]	Expt.[b]
CO					
5σ	15.10	13.99	14.19	13.95	14.01
1π	17.43	17.02	17.10	17.03	16.91
4σ	21.90	20.17	19.80	19.60	19.72
F_2					
$1\pi_g$	18.16	16.04	15.63	15.69	15.83
$1\pi_u$	22.10	19.23	18.97	18.89	18.8
$3\sigma_g$	20.49	20.97	21.19	21.11	21.1
N_2					
$3\sigma_g$	17.27	15.79	15.66	15.54	15.60
$1\pi_u$	16.72	16.90	17.27	16.99	16.98
$2\sigma_u$	21.22	19.07	18.91	18.74	18.78
$\bar{\Delta}_{abs}$	1.31	0.17	0.13	0.06	
Δ_{max}	3.30	0.45	0.29	0.14	

[a]IP-EOM-CC results for aug-cc-pVTZ basis set Ref. 34.
[b]Experimental vertical ionization energies from Ref. 47.

3. Comparison with CC results

In Table IV we compare the vertical ionization energies of CO, F_2, and N_2 computed using the nD-ADC(3) scheme with IP-EOM-CCSD and IP-EOM-CCSDT results[34] and experimental data from Ref. 47.

The mean error of the nD-ADC(3) scheme relative to experiment is 0.17 eV, which is consistent with the findings in Table II. The IP-EOM-CCSD results, the mean error being 0.13 eV, appear to be slightly more accurate. It should be noted that the better performance of the IP-EOM-CCSD method here may not reflect a systematic trend because in contrast to the ADC(3) scheme, that CC scheme is not a consistent third-order method. Moreover one should recall that computationally the IP-EOM-CCSD method is by an order of magnitude more expensive than the nD-ADC(3) (see Table I).

The IP-EOM-CCSDT treats single-hole states consistently through third order. Clearly, this scheme provides distinctly more accurate results than the nD-ADC(3) method. The superior performance of the IP-EOM-CCSDT is obviously related to the fact that it goes in many respects beyond the nD-ADC(3) level; the ground state here is treated through fourth order and the $1p$-$2h$ configurations (often playing important role in the final states) are treated through second order. However, the computational costs of the IP-EOM-CCSDT are also much higher than in the nD-ADC(3) (Table I).

TABLE V. Comparison of vertical ionization energies (eV) obtained using various second- and third-order nD-ADC schemes. The last two lines give the mean absolute error $\bar{\Delta}_{abs}$ and the maximum absolute error Δ_{max} relative to the experimental data (eV).

System, $1h$ configuration	ADC(2)	ADC(2)-E	ADC(3)[a] $\Sigma(3)$	$\Sigma(4)$	$\Sigma(4+)$	Σ(DEM)	Expt.[b]
C_2H_4							
$1b_{2u}$	10.15	10.09	10.45	10.51	10.49	10.46	10.95
$1b_{2g}$	12.79	12.57	13.21	13.23	13.20	13.19	12.95
$3a_g$	13.79	13.67	14.33	14.40	14.37	14.36	14.88
$1b_{3u}$	16.13	15.61	16.50	16.52	16.50	16.49	16.34
		18.08	18.12	18.12	18.12	18.12	17.8
$2b_{1u}$	18.96	18.08	19.00	19.02	19.01	19.00	19.4
		19.92	20.02	20.02	20.02	20.02	20.45
CO							
5σ	13.78	13.43	13.58	14.04	13.87	13.80	14.01
1π	16.23	16.30	17.12	16.59	16.88	16.88	16.91
4σ	18.30	18.42	20.45	19.69	20.09	20.10	19.72
F_2							
$1\pi_g$	13.88	13.97	16.00	15.80	15.86	15.87	15.8
$1\pi_u$	17.03	16.84	19.23	19.05	19.09	19.11	18.8
$3\sigma_g$	20.24	20.48	21.22	20.98	21.03	21.01	21.1
HF							
1π	14.39	14.93	16.77	16.17	16.39	16.41	16.1
3σ	18.67	19.11	20.63	20.09	20.28	20.30	20.0
N_2							
$3\sigma_g$	14.79	14.72	15.41	15.68	15.62	15.60	15.60
$1\pi_u$	16.99	16.90	16.57	16.85	16.79	16.77	16.98
$2\sigma_u$	17.99	17.62	18.80	19.00	18.95	18.93	18.78
$\bar{\Delta}_{abs}$[c]	0.89	0.97	0.37	0.20	0.23	0.24	
Δ_{max}[c]	1.95	1.96	0.73	0.48	0.51	0.52	

[a]nD-ADC(3) schemes differing by the treatment of the self-energy $\mathbf{\Sigma}(\infty)$ contributions (see text for details).
[b]Experimental vertical ionization energies for C_2H_4 are from Ref. 44; the remaining data are from Ref. 47.
[c]Only transitions with dominant single-hole character are taken into account (i.e., transitions of C_2H_4 with experimental ionization energies 17.8 and 20.45 eV are omitted).

B. Comparison of various ADC schemes

In this section we discuss in more detail the nD-ADC(2) and nD-ADC(3) schemes and some variants concerning the treatment of the constant self-energy contributions. In Table V the vertical ionization energies of C_2H_4, CO, F_2, HF, and N_2 obtained at various ADC levels are compared with each other and with the experimental data.

As seen from Table V, both the strict and the extended nD-ADC(2) schemes yield a similar level of accuracy for the single-hole states. The mean absolute error here is 0.9–1.0 eV, but maximum errors up to 2.0 eV can occur. The advantage of the extended [nD-ADC(2)-E] scheme becomes apparent for the transitions with dominant $1p$-$2h$ character (e.g., transitions of C_2H_4 with the experimental energies of 17.8 and 20.45 eV). Transitions of this type, being only poorly described at the strict nD-ADC(2) level, are much better represented by the nD-ADC(2)-E scheme.

The ionization energies of nD-ADC(3) variants associated with different treatments of $\mathbf{\Sigma}(\infty)$ differ from each other in the order of the typical third-order error ($\leqslant$0.2–0.3 eV). The largest differences here can be seen between the third- and the improved fourth-order treatments. Whereas the average error of the $\Sigma(3)$ scheme is about 0.4 eV, it is reduced to 0.2–0.3 eV, when a $\mathbf{\Sigma}(\infty)$ treatment beyond third order is employed. An important observation is that the Σ(DEM) and $\Sigma(4+)$ schemes yield virtually identical results. The maximal differences between the individual ionization energies of these methods is only 0.06 eV. This suggests that the $\Sigma(4+)$ approximation can successfully substitute the computationally more involved Σ(DEM) treatment.

C. Static self-energy

In view of the importance of $\mathbf{\Sigma}(\infty)$ for the overall accuracy of the nD-ADC(3) scheme, it is useful to take a direct look to this quantity and the results of its various approximations. The results in Table VI demonstrate a considerable magnitude of many diagonal $\Sigma_{kk}(\infty)$ terms. Especially large values are found in CO, CS, F_2, HF, and H_2CO reflecting large differences between the HF and the correlated ground-

TABLE VI. Results for diagonal static self-energy $\Sigma_{kk}(\infty)$ (eV) contributions at different levels of theory. The last two lines give the mean absolute error $\bar{\Delta}_{abs}$ and the maximum absolute error Δ_{max} relative to the Dyson-expansion method Σ(DEM). See Sec. II B for details. Computational framework as in the case of Table II.

System, orbital	$\Sigma(3)$	$\Sigma(4)$	$\Sigma(4+)$	Σ(DEM)
C_2H_4				
$1b_{2u}$	0.34	0.28	0.30	0.34
$1b_{2g}$	0.29	0.27	0.30	0.32
$3a_g$	0.39	0.31	0.35	0.36
$1b_{3u}$	0.26	0.23	0.25	0.27
CO				
5σ	0.88	0.38	0.58	0.65
1π	−0.21	0.37	0.06	0.05
4σ	−0.54	0.35	−0.11	−0.13
CS				
7σ	0.26	0.29	0.26	0.26
2π	1.12	0.36	0.73	0.79
6σ	0.27	0.35	0.29	0.30
F_2				
$1\pi_g$	−0.19	0.03	−0.03	−0.05
$1\pi_u$	−0.14	0.13	0.07	0.10
$3\sigma_g$	−0.21	0.01	−0.05	−0.07
H_2CO				
$2b_2$	−0.15	0.23	0.02	0.02
$1b_1$	−0.11	0.22	0.07	0.07
$5a_1$	−0.21	0.20	−0.03	−0.05
$1b_2$	0.21	0.21	0.22	0.22
H_2O				
$1b_1$	−0.27	0.05	−0.05	−0.07
$3a_1$	−0.29	0.02	−0.08	−0.10
$1b_2$	−0.27	0.00	−0.09	−0.10
HF				
1π	−0.68	−0.05	−0.28	−0.30
3σ	−0.59	−0.04	−0.24	−0.26
N_2				
$3\sigma_g$	0.60	0.31	0.37	0.39
$1\pi_u$	0.70	0.41	0.47	0.50
$2\sigma_u$	0.59	0.35	0.40	0.42
Ne				
$2p$	−0.38	−0.06	−0.15	−0.16
$\bar{\Delta}_{abs}$	0.17	0.14	0.02	
Δ_{max}	0.41	0.48	0.07	

state electron density in these systems. The third-order $\Sigma_{kk}(\infty)$ values, for example, amount in some case to 1 eV ($2\pi^{-1}$ transition of CS).

The individual $\Sigma_{kk}(\infty)$ values change substantially when going from the third- to the fourth-order level. Here changes up to 1 eV ($4\sigma^{-1}$ transition of CO) and even alternations of the sign can be seen. The results of the fourth-order schemes including the DEM scheme are more consistent with each other. Here the changes of individual $\Sigma_{kk}(\infty)$ values do not exceed 0.5 eV.

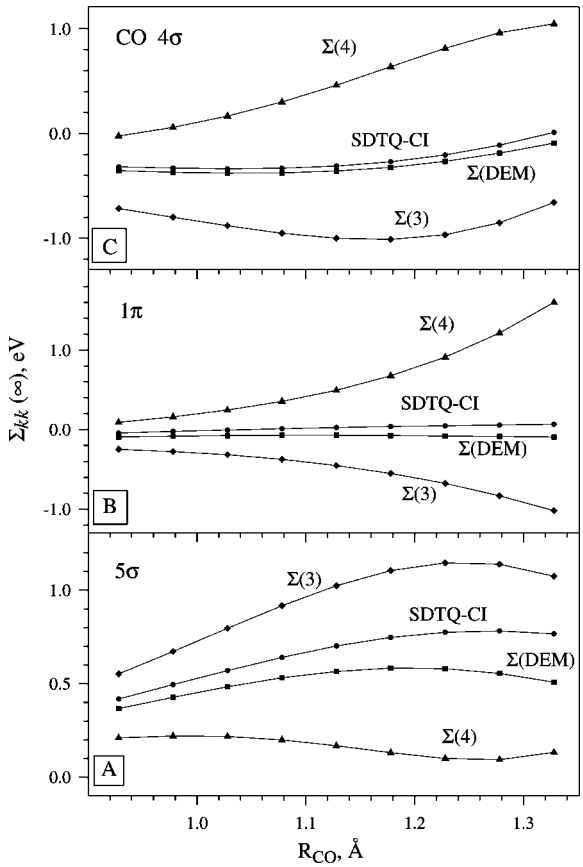

FIG. 2. Diagonal elements $\Sigma_{kk}(\infty)$ of the static-self energy in CO as a function of the internuclear distance at various approximate levels (see text for details).

To assess the performance of various $\mathbf{\Sigma}(\infty)$ treatments we compare in Table VI the corresponding results to the results of the DEM, which is viewed as the best available treatment. From this analysis it is evident that the $\Sigma(4+)$ scheme is an excellent approximation to the DE method. According to the present statistics, comprising 27 transitions in 9 systems, the mean and maximum error of the $\Sigma(4+)$ scheme relative to the Σ(DEM) scheme is 0.02 and 0.07 eV, respectively. The strict third- and third-plus-fourth-order treatments, $\Sigma(3)$ and $\Sigma(4)$, show distinctly larger errors.

The results of Table VI do not allow to assess the absolute accuracy of the $\mathbf{\Sigma}(\infty)$ treatments being compared. The latter can be established only through comparison with the results of suitable benchmark calculations. To obtain such $\mathbf{\Sigma}(\infty)$ benchmarks, we performed CI calculations including all single, double, triple, and quadruple excitations (SDTQ-CI) for CO. The corresponding one-particle density matrices were employed in Eq. (17) to evaluate $\mathbf{\Sigma}(\infty)$. To make this accuracy test more informative, we consider in Fig. 2 these results as a function of the internuclear separations. The outermost molecular orbitals (MO) 5σ, 1π, and 4σ of CO are considered.

As seen from Fig. 2, the $\Sigma_{kk}(\infty)$ curves of the DEM scheme are closely parallel to the SDTQ-CI curves. The DEM error increases slightly with the internuclear separation amounting to 0.2–0.3 eV at the end of the considered range. The $\Sigma(4+)$ curve, not shown in Fig. 2, nearly coincides with

TABLE VII. Comparison of vertical ionization energies (eV) obtained using nD-ADC(3) scheme and various basis sets. Equilibrium ground-state geometry and calculations for CO, N_2, and F_2 as in Ref. 34, for HF as in Table II. Only transitions with dominant single-hole character are shown. The last two lines give the mean absolute error $\bar{\Delta}_{abs}$ and the maximum absolute error Δ_{max} relative to the experimental data (eV).

System, $1h$ configuration	cc-pVDZ	aug-cc-pVDZ	cc-pVTZ	aug-cc-pVTZ	Expt.[a]
CO					
5σ	13.59	13.79	13.92	13.99	14.01
1π	16.67	16.90	16.94	17.02	16.91
4σ	19.89	20.10	20.10	20.17	19.72
N_2					
$3\sigma_g$	15.31	15.59	15.70	15.79	15.60
$1\pi_u$	16.56	16.79	16.80	16.90	16.98
$2\sigma_u$	18.68	18.91	18.98	19.07	18.78
F_2					
$1\pi_g$	15.45	15.89	15.87	16.03	15.83
$1\pi_u$	18.64	19.12	19.05	19.23	18.8
$3\sigma_g$	20.50	21.03	20.79	20.97	21.1
HF					
1π	15.68	16.41	16.31	16.55	16.05
3σ	19.58	20.30	20.07	20.32	20.0
$\bar{\Delta}_{abs}$	0.32	0.19	0.17	0.25	
Δ_{max}	0.60	0.38	0.38	0.50	

[a]Experimental vertical ionization energies from Ref. 47.

the Σ(DEM) curve. Clearly, the $\Sigma(3)$ and $\Sigma(4)$ curves depart considerably from the SDTQ-CI curve especially at larger CO distances. The strongest divergence is observed in case of the 1π MO amounting to 1.1 eV. Interestingly, the strict third-plus-fourth-order treatment $\Sigma(4)$ does not yield an improvement with respect to the third-order scheme, inverting only the error sign relative to SDTQ-CI.

The conclusion to be drawn from this discussion is that the $\Sigma(4+)$ approximation is an excellent surrogate for the computationally much more expensive DEM procedure. The $\Sigma(4+)$ scheme uses only computational input provided anyway at the nD-ADC(3) level and does not require one to deal with the $2p$-$1h$ configurations of $N+1$ electrons. This qualifies the $\Sigma(4+)$ approximation as the natural ingredient of the nD-ADC(3) method.

D. Basis set effect on third-order ionization energies

In Table VII we study the basis set effect on the nD-ADC(3) ionization energies. The results obtained using the cc-pVDZ, aug-cc-pVDZ, cc-pVTZ, and aug-cc-pVTZ (Ref. 64) basis sets of improving quality are compared.

As seen from Table VII, there is a distinct improvement of the results between the cc-pVDZ and aug-cc-pVDZ levels. Only for the $4\sigma^{-1}$ transition in the CO the agreement with experiment becomes somewhat worse. The ionization energies change on the average by about 0.4 eV from the cc-pVDZ to the aug-cc-pVDZ basis. Similar changes can be seen when going from the cc-pVDZ to cc-pVTZ basis. The accuracy of the results at the aug-cc-pVDZ and cc-pVTZ levels is nearly the same (the average and maximum error in both cases is 0.2 and 0.4 eV, respectively) and distinctly better than at the cc-pVDZ level (the average and maximum error is 0.3 and 0.6 eV, respectively).

A further extension of the basis set from the cc-pVTZ to the aug-cc-pVTZ level improves the results only rather selectively. The ionization energies change on the average by 0.1 eV, that is, much less than at the previous step. The observed changes are comparable to (or even less than) the error of the nD-ADC(3) scheme itself. It is clear that one cannot expect the basis set to improve the results beyond the intrinsic ADC(3) error of about 0.2 eV.

E. Ground-state properties: Dipole moments

The dipole moment is a convenient example for the discussion of one-electron GS properties. The experimental dipole moments are known to good accuracy for many molecules. They can also routinely be calculated using standard quantum chemical methods. In the latter case, usually the evaluation of the GS one-particle density matrix is presupposed. The dipole moments are then computed according to Eq. (21). The same approach is also used in the present case where the density matrix is given by Eq. (19). [As in the treatment of the static self-energy part $\boldsymbol{\Sigma}(\infty)$, there are several options for the evaluation of $\boldsymbol{\rho}$ at the ADC(3) level referred to as $\Sigma(3)$, $\Sigma(4)$, $\Sigma(4+)$, and Σ(DEM).] In Table VIII we show the present nD-ADC(2) and nD-ADC(3) GS dipole moments for five molecules in comparison with the MRCI results (see Sec. III) and experimental data.[48–52] The nD-

TABLE VIII. Ground-state dipole moments (D) obtained using HF, various nD-ADC schemes, and the MRCI methods (z component). The last two lines gives the mean absolute error $\bar{\Delta}_{abs}$ and the maximum absolute error Δ_{max} relative to MRCI.

			ADC(3)					
Molecule	HF	ADC(2)	$\Sigma(3)$	$\Sigma(4)$	$\Sigma(4+)$	Σ(DEM)	MRCI	Expt.[a]
CO	−0.26	0.45	−0.16	0.27	0.07	0.06	0.12	0.11
CS	1.55	2.47	1.42	2.41	1.96	1.95	1.96	1.97
H_2CO	2.81	2.21	2.58	2.31	2.40	2.41	2.38	2.33
H_2O	2.00	1.83	1.90	1.87	1.88	1.88	1.87	1.85
HF	1.93	1.76	1.85	1.80	1.82	1.82	1.80	1.84
$\bar{\Delta}_{abs}$	0.30	0.22	0.22	0.13	0.02	0.03		
Δ_{max}	0.43	0.51	0.54	0.45	0.05	0.06		

[a]Experimental data: CO (Ref. 48), CS (Ref. 49), H_2CO (Ref. 50), H_2O (Ref. 51), and HF (Ref. 52).

ADC(2) scheme allows one to obtain the second-order density matrix. This is the first nontrivial approximation for $\boldsymbol{\rho}$, which, as seen from Table VIII, provides almost no improvement for the calculated GS dipole moments with respect to the HF level. The situation is not improved by the nD-ADC(3) scheme using $\boldsymbol{\Sigma}(3)$. Some improvement is obtained when the strict third-plus-fourth-order treatment of $\boldsymbol{\Sigma}(\infty),\Sigma(4)$, is employed. An oscillatory behavior of the μ values with respect to the order of $\boldsymbol{\Sigma}(\infty)$ treatment can be noted for molecules with strong GS electron correlation effects such as CO, CS, and H_2CO. The agreement with MRCI and experimental data improves considerably at the extended fourth-order $\Sigma(4+)$ and $\tilde{\Sigma}(\mathrm{DEM})$ levels. The differences between the latter two schemes are negligible. The agreement with MRCI and experiment at this stage is very good for all molecules. These examples indicate that the ground-state density ρ, as $\boldsymbol{\Sigma}(\infty)$, has often slow and oscillating convergence so that treatments beyond third order have to be used in order to ensure meaningful results for one-electron properties.

V. SUMMARY AND CONCLUSIONS

The comprehensive numerical tests performed in the present work for the non-Dyson (nD) electron propagator ADC(3) method[24] have shown that this method represents a useful alternative to the original Dyson ADC(3) method.[14,21] Whereas the nD-ADC(3) and Dyson ADC(3) methods are nearly identical with respect to numeric results, the former method has the advantage that the $(N\pm1)$-electron parts of one-particle Green's function are decoupled from each other, and the corresponding equations can be solved separately. This enables a very efficient computer implementation of the method, which scales as n^5 with respect to the number of molecular orbitals n and ensures fast convergence of the iterative (Davidson or Lanczos) diagonalization techniques to the lowest ionization energies. This is because the corresponding eigenvalues are no longer "buried" in the middle of the spectrum, as in the Dyson ADC(3) case, but located within the more easily accessible margin region.

The nD-ADC(3) method combines diagonalization of a Hermitian secular matrix with perturbation theory for the matrix elements. The explicit configuration space here is spanned by $1h$ and $1p$-$2h$ configurations. As a consequence of the so-called compactness property, the nD-ADC(3) results for the single-hole ionization are consistent through third order in the residual electronic repulsion. The nD-ADC(3) secular matrix is separable, which leads to size-intensive results both for ionization energies and corresponding spectroscopic factors. Like the CC methods the nD-ADC(3) allows for "black-box computations."

As established in the present study, the absolute accuracy of the nD-ADC(3) vertical ionization energies associated with single-hole ionization processes is 0.2–0.3 eV with respect to both experimental and FCI results. The comparison with FCI yields somewhat better accuracy estimates, which reflects difficulties with the experimental determination of vertical ionization energies. In some cases errors up to 0.5–0.7 eV were found, mainly in systems where difficulties arise in the perturbative treatment of the electronic ground state. The accuracy of the nD-ADC(3) is comparable to that of the IP-EOM-CCSD.[34] The IP-EOM-CCSD, however, is not a consistent third-order method and has scaling properties one order of magnitude worse than the nD-ADC(3).

The strict and extended second-order [nD-ADC(2)] schemes were tested as well. Here, the accuracy of single-hole ionization energies is about 0.9–1.0 eV. In general, the nD-ADC(2) and nD-ADC(2)-E schemes improve the HF results, but their accuracy is still insufficient for most spectroscopic applications. The second-order schemes can be recommended for qualitative studies especially of the larger systems.

An essential factor for the performance of the nD-ADC(3) method is the improved treatment of contributions arising from the so-called static self-energy $\boldsymbol{\Sigma}(\infty)$ part. The best available treatment of $\boldsymbol{\Sigma}(\infty)$ is the Dyson-expansion method,[21] which provides a consistent fourth-order description of $\boldsymbol{\Sigma}(\infty)$ with additional partial infinite summation of higher-order terms. The DEM treatment of $\boldsymbol{\Sigma}(\infty)$ can readily be adopted for the nD-ADC(3) scheme, but, as has been shown in the present work, it is preferable both from a computational and methodological point of view to employ instead the $\Sigma(4+)$ approach based on the Eqs. (17)–(19). The latter approach, staying strictly within the nD concept, provides an improved fourth-order treatment of $\boldsymbol{\Sigma}(\infty)$ and yields results which are very similar to those of the DE method.

The nD-ADC formalism allows for a direct access to the one-particle GS density matrix $\boldsymbol{\rho}$ according to Eq. (19), which can be used to compute ground-state one-electron properties in a standard way. As has been demonstrated in the present work for the GS dipole moments, this procedure leads to excellent results, when an extended fourth-order treatment of $\boldsymbol{\Sigma}(\infty)$ is employed.

In contrast to other propagator methods, the nD-ADC approach is not restricted to the treatment of GS properties. The ISR formulation, as outlined in Sec. III D, allows one to exploit the full potential of a wave-function approach: the method can readily be extended to the computation of ionic-state one-particle properties and transition moments.[53] The required ISR equations, derived in this work, are presented in Appendix B. It should be noted that first applications of these ISR ionic-state properties have been reported in Ref. 70.

The nD-ADC(3) is thus a versatile and computationally practical method having several important advantages over the previous Dyson ADC version. It is to be expected that the nD-ADC(3) scheme will become a standard computational tool in the near future replacing the original ADC(3) method. An efficient implementation fully exploiting the n^5 potential should enable applications to rather large systems. As a step in this direction, a more advanced version of the nD-ADC(3) code (yet being organized conventionally) has already been written[71] and is presently tested in medium size applications (e.g., SiF_4 molecule using the aug-cc-pVTZ basis).[72] The calculations confirm the superior efficiency of the nD-ADC(3) method with respect to the Dyson ADC(3), in particular, in the diagonalization step.

The transparent computational scheme of the nD-ADC method is very appealing for various theoretical extensions.

One of such extensions is the adoption of the nD-ADC schemes for Dirac-Fock relativistic calculations.[73] Another interesting possibility concerns applications of the present intermediate-state representation of one-particle operators. As discussed in Ref. 53, this enables an elegant ADC treatment of Hamiltonians including various one-particle perturbation operators. In this way, for example, a complex absorption potential (CAP) used for the evaluation of lifetimes of electronic states[74] can easily be incorporated into the present nD-ADC electron propagator formalism.

ACKNOWLEDGMENTS

The authors thank A. Thiel for assistance in the SDTQ-CI calculations and J. Breidbach for various cooperations. This work was supported by the Deutsche Forschungsgemeinschaft (DFG) and by the Russian Foundation for Basic Research (RFBR). One of the authors (A.B.T.) gratefully acknowledges a grant of the Federal Agency for Education.

APPENDIX A: EXPLICIT ADC(3) EXPRESSIONS

In the following we collect the expressions for the elements of the effective interaction matrix $\mathbf{K}+\mathbf{C}$ and the matrix of effective transition moments, $\mathbf{f}$. As mentioned in Sec. II A, the third-order ADC expressions can be written in a symmetric form, namely, so that the $1h$ block of $\mathbf{f}$ is Hermitian. (Note that the secular matrix $\mathbf{K}+\mathbf{C}$ is always Hermitian.) This follows from the ADC procedure, which allows one to shift any anti-Hermitian contributions in the $1h$ block of $\mathbf{f}$ into nondiagonal contributions of the $1h/1h$ block of $\mathbf{C}$.[24] The Hermitian-$\mathbf{f}$ expressions presented here are as legitimate as the original nD-ADC(3) expressions derived in Ref. 24. The single-hole ionization energies of the two forms differ by sixth-order contributions. In the present computations the numerical differences never exceeded 0.01 eV. Due to their higher symmetry with respect to the one-particle indices, the Hermitian-$\mathbf{f}$ expressions are more advantageous in the computer implementation. Only matrix elements $C^{(3)}_{pp'}$ and $f^{(3)}_{pp'}$ differing from those in Ref. 24 are given below. For brevity we use the notation

$$\nu_{pqrs} = \frac{V_{pq[rs]}}{\varepsilon(pqrs)}, \tag{A1}$$

where $V_{pq[rs]}=V_{pqrs}-V_{pqsr}$ denote antisymmetrized Coulomb integrals in 1212 notation and $\varepsilon(pqrs)=\varepsilon_p+\varepsilon_q-\varepsilon_r-\varepsilon_s$ denote combinations of the HF orbital energies. As before, the subscripts $i,j,k,\ldots$, and $a,b,c,\ldots$, refer to occupied and unoccupied orbitals, respectively. The subscript $p,q,r,\ldots$, label both occupied and unoccupied orbitals.

1. The $(N-1)$-electron case

a. Effective interaction

$$C^{(3)}_{kk'} = C^{(A)}_{kk'} + C^{(B)}_{kk'} + C^{(C)}_{kk'} + C^{(D)}_{kk'} + \Sigma^{(3)}_{k'k}(\infty), \tag{A2}$$

where

$$C^{(A)}_{kk'} = \frac{1}{8}\sum_{\substack{a,b,c,d\\ l}} V_{ab[kl]}V^{*}_{cd[k'l]}V_{cd[ab]}\left(\frac{1}{\varepsilon(ablk)\varepsilon(cdlk)} + \frac{1}{\varepsilon(ablk')\varepsilon(cdlk')}\right), \tag{A3}$$

$$C^{(B)}_{kk'} = \frac{1}{2}\sum_{\substack{a,b,c\\ l,m}} V_{ab[kl]}V^{*}_{ac[k'm]}V_{lc[bm]}\left(\frac{1}{\varepsilon(ablk)\varepsilon(acmk)} + \frac{1}{\varepsilon(ablk')\varepsilon(acmk')}\right), \tag{A4}$$

$$C^{(C)}_{kk'} = \frac{1}{4}\sum_{\substack{a,b\\ l,m,j}} \nu_{ablm}\nu^{*}_{abjk'}V_{lm[jk]} \times\left(\frac{\varepsilon_a+\varepsilon_b-\varepsilon_j-(1/2)\varepsilon_k-(1/2)\varepsilon_{k'}}{\varepsilon(abjk)}\right)+\text{h.c.}, \tag{A5}$$

$$C^{(D)}_{kk'} = \sum_{\substack{a,b,c\\ l,m}} \nu_{ablm}\nu^{*}_{bck'm}V_{lc[ka]}\left(\frac{\varepsilon_b+\varepsilon_c-\varepsilon_m-\frac{1}{2}\varepsilon_k-\frac{1}{2}\varepsilon_{k'}}{\varepsilon(bcmk)}\right) + \text{h.c.} \tag{A6}$$

The self-energy part $\Sigma^{(3)}_{k'k}(\infty)$ is obtained as described in Ref. 24.

b. Effective transition moments

$$f^{(3)}_{kk'} = f^{(A)}_{kk'} + f^{(B)}_{kk'} + f^{(C)}_{kk'} + f^{(D)}_{kk'}, \tag{A7}$$

where

$$f^{(A)}_{kk'} = \frac{1}{8}\sum_{\substack{a,b,c,d\\ l}} \nu_{abkl}\nu^{*}_{cdk'l}V_{cd[ab]}\left(\frac{1}{\varepsilon(ablk')}+\frac{1}{\varepsilon(cdlk)}\right), \tag{A8}$$

$$f^{(B)}_{kk'} = \frac{1}{2}\sum_{\substack{a,b,c\\ l,m}} \nu_{abkl}\nu^{*}_{ack'm}V_{lc[bm]}\left(\frac{1}{\varepsilon(ablk')}+\frac{1}{\varepsilon(acmk)}\right), \tag{A9}$$

$$f^{(C)}_{kk'} = \frac{1}{8}\sum_{\substack{a,b\\ l,m,j}} \nu_{ablm}\nu^{*}_{abjk'}V_{lm[jk]}\frac{1}{\varepsilon(abjk)}+\text{h.c.}, \tag{A10}$$

$$f^{(D)}_{kk'} = \frac{1}{2}\sum_{\substack{a,b,c\\ l,m}} \nu_{ablm}\nu^{*}_{bck'm}V_{lc[ka]}\frac{1}{\varepsilon(bcmk)}+\text{h.c.} \tag{A11}$$

2. The $(N+1)$-electron case

The Hermitian-$\mathbf{f}$ expressions for the matrix elements of the effective interaction matrix $\mathbf{K}+\mathbf{C}$ and the matrix of effective transition moments, $\mathbf{f}$, for the $\mathbf{G}^{+}(\omega)$ or

$(N+1)$-electron part of the one-particle Green's function can be obtained from the above expressions using the rules described in Appendix B of Ref. 24.

APPENDIX B: SECOND-ORDER $(N\pm1)$-ELECTRON INTERMEDIATE-STATE REPRESENTATION OF ONE-PARTICLE OPERATORS

In the following we collect the explicit expressions for the matrix elements of a general one-particle operator

$$\hat{D} = \sum_{r,s} d_{rs} c_r^\dagger c_s \tag{B1}$$

with respect to the second-order $(N\pm1)$-electronic intermediate states $|\tilde{\Psi}_J^{N\pm1}\rangle$:[27,28,53]

$$\tilde{D}_{IJ} = \langle \tilde{\Psi}_I^{N\pm1} | \hat{D} | \tilde{\Psi}_J^{N\pm1} \rangle. \tag{B2}$$

The same notations as in Appendix A are used.

1. The $(N-1)$-electron case

a. h/h diagonal block

$$\tilde{D}_{i,i'} = \delta_{ii'} D_0(2) - d_{i'i} - \sum_c (\rho_{ic}^{(2)} d_{i'c} + \rho_{ci'}^{(2)} d_{ci}) + \sum_{\mu=1}^{3} \tilde{D}_{i,i'}^{(2,\mu)}, \tag{B3}$$

where the contributions $\tilde{D}_{i,i'}^{(2,\mu)}$ are given by

$$\tilde{D}_{i,i'}^{(2,1)} = -\sum_{\substack{n \\ b,f,g}} \nu_{fbi'n}^* \nu_{fgin} d_{bg}, \tag{B4}$$

$$\tilde{D}_{i,i'}^{(2,2)} = \frac{1}{2} \sum_{\substack{n,j \\ f,g}} \nu_{fgi'j}^* \nu_{fgin} d_{nj}, \tag{B5}$$

$$\tilde{D}_{i,i'}^{(2,3)} = -\frac{1}{4} \sum_{\substack{n,j \\ f,g}} \nu_{fgnj}^* \nu_{fgin} d_{i'j} + \text{h.c.} \tag{B6}$$

b. h/1p-2h coupling block

$$\tilde{D}_{i,a'i'j'} = \delta_{ij'} d_{i'a'} - \delta_{ii'} d_{j'a'} + \delta_{ii'} \sum_{ck} \nu_{ca'kj}^* d_{ck} - \delta_{ij'} \sum_{ck} \nu_{ca'ki'}^* d_{ck} - \sum_c \nu_{ca'i'j'}^* d_{ci}. \tag{B7}$$

c. 1p-2h/1p-2h diagonal block

$$\tilde{D}_{aij,a'i'j'} = \delta_{aa'} \delta_{ii'} \delta_{jj'} D_0(0) + \delta_{ii'} \delta_{jj'} d_{aa'} - \delta_{aa'} \delta_{ii'} d_{j'j} + \delta_{aa'} \delta_{ij'} d_{i'j} - \delta_{aa'} \delta_{jj'} d_{i'i} + \delta_{aa'} \delta_{ji'} d_{j'i}. \tag{B8}$$

2. The $(N+1)$-electron case

a. p/p diagonal block

$$\tilde{D}_{a,a'} = \delta_{aa'} D_0(2) + d_{aa'} - \sum_l (\rho_{la}^{(2)} d_{la'} + \rho_{a'l}^{(2)} d_{al}) + \sum_{\mu=1}^{3} \tilde{D}_{a,a'}^{(2,\mu)}, \tag{B9}$$

where the contributions $\tilde{D}_{a,a'}^{(2,\mu)}$ are given by

$$\tilde{D}_{a,a'}^{(2,1)} = \sum_{\substack{m,n,k \\ g}} \nu_{a'gkn}^* \nu_{agmn} d_{mk}, \tag{B10}$$

$$\tilde{D}_{a,a'}^{(2,2)} = \frac{1}{2} \sum_{\substack{m,n \\ c,g}} \nu_{ca'mn}^* \nu_{agmn} d_{cg}, \tag{B11}$$

$$\tilde{D}_{a,a'}^{(2,3)} = -\frac{1}{4} \sum_{\substack{m,n \\ c,g}} \nu_{cgmn}^* \nu_{agmn} d_{ca'} + \text{h.c.} \tag{B12}$$

b. p/2p-1h coupling block

$$\tilde{D}_{a,a'b'i'} = \delta_{aa'} d_{i'b'} - \delta_{ab'} d_{i'a'} - \delta_{aa'} \sum_{ck} \nu_{cb'ki'}^* d_{ck} + \delta_{ab'} \sum_{ck} \nu_{ca'ki'}^* d_{ck} + \sum_k \nu_{a'b'ki'}^* d_{ak}. \tag{B13}$$

c. 2p-1h/2p-1h diagonal block

$$\tilde{D}_{abi,a'b'i'} = \delta_{aa'} \delta_{bb'} \delta_{ii'} D_0(0) - \delta_{aa'} \delta_{bb'} d_{i'i} + \delta_{bb'} \delta_{ii'} d_{aa'} - \delta_{ba'} \delta_{ii'} d_{ab'} + \delta_{aa'} \delta_{ii'} d_{bb'} - \delta_{ab'} \delta_{ii'} d_{ba'}. \tag{B14}$$

In the above expressions, $D_0(2)$ and $D_0(0)$ denote the ground-state dipole moment consistent through second and zeroth orders of perturbation theory, respectively; $\rho_{ic}^{(2)}$ denotes second-order contributions to the one-particle density-matrix elements.

[1] A. L. Fetter and J. D. Walecka, *Quantum Theory of Many-Particle Systems* (McGraw-Hill, New York, 1971).
[2] A. A. Abrikosov, L. P. Gorkov, and I. E. Dzyaloshinski, *Methods of Quantum Field Theory in Statistical Physics* (Prentice-Hall, Englewood Cliffs, 1963).
[3] L. S. Cederbaum and W. Domcke, Adv. Chem. Phys. **36**, 205 (1977).
[4] J. Simons, Annu. Rev. Phys. Chem. **28**, 1 (1977).
[5] J. Oddershede, Adv. Quantum Chem. **11**, 275 (1978).
[6] M. F. Herman, K. F. Freed, and D. L. Yeager, Adv. Chem. Phys. **48**, 1 (1981).
[7] Y. Öhrn and G. Born, Adv. Quantum Chem. **13**, 1 (1981).
[8] W. von Niessen, J. Schirmer, and L. S. Cederbaum, Comput. Phys. Rep. **1**, 59 (1984).
[9] L. S. Cederbaum, W. Domcke, J. Schirmer, and W. von Niessen, Adv. Chem. Phys. **65**, 115 (1986).
[10] J. V. Ortiz, V. G. Zakrzewski, and O. Dolgounitcheva, in *Conceptual Trends in Quantum Chemistry*, edited by E. Kryachko (Kluwer, Dordrecht, 1997), Vol. 3; J. V. Ortiz, in *Computational Chemistry: Reviews of Current Trends*, edited by J. Leszczyinski (World Scientific, Singapore, 1997), Vol. 2; J. V. Ortiz, J. Chem. Phys. **104**, 7599 (1996); J. Chem. Phys. **108**, 1008 (1998).

[11] P. Jørgensen and J. Simons, *Second Quantization-Based Methods in Quantum Chemistry* (Academic, New York, 1981).
[12] R. McWeeny, *Methods of Molecular Quantum Mechanics* (Academic, London, 1989).
[13] J. Schirmer, Phys. Rev. A **26**, 2395 (1982).
[14] J. Schirmer, L. S. Cederbaum, and O. Walter, Phys. Rev. A **28**, 1237 (1983).
[15] D. J. Rowe, Rev. Mod. Phys. **40**, 153 (1968).
[16] C. W. McCurdy, T. N. Rescigno, D. L. Yeager, and V. McKoy, in *Methods of Electronic Structure Theory*, edited by H. F. Schaefer (Plenum, New York, 1977).
[17] D. Goscinski and B. Lukman, Chem. Phys. Lett. **7**, 573 (1970).
[18] B. T. Pickup and O. Goscinski, Mol. Phys. **26**, 19 (1973).
[19] P. Jørgensen, Annu. Rev. Phys. Chem. **26**, 359 (1975).
[20] L. S. Cederbaum, J. Phys. B **8**, 290 (1975).
[21] J. Schirmer and G. Angonoa, J. Chem. Phys. **91**, 1754 (1989).
[22] H.-G. Weikert, H.-D. Meyer, and L. S. Cederbaum, J. Chem. Phys. **104**, 7122 (1996).
[23] D. M. P. Holland, M. A. MacDonald, P. Baltzer, L. Karlsson, M. Lundqvist, B. Wannberg, and W. von Niessen, Chem. Phys. **192**, 333 (1995); D. M. P. Holland, M. A. MacDonald, M. A. Hayes, P. Baltzer, B. Wannberg, M. Lundqvist, L. Karlsson, and W. von Niessen, J. Phys. B **29**, 3091 (1996); O. Dolgounitcheva, V. G. Zakrzewski, and J. V. Ortiz, J. Phys. Chem. A **104**, 10032 (2000); O. Dolgounitcheva, V. G. Zakrzewski, and J. V. Ortiz, J. Chem. Phys. **114**, 130 (2001); M. S. Deleuze, A. B. Trofimov, and L. S. Cederbaum, *ibid.* **115**, 5859 (2001); M. S. Deleuze, *ibid.* **116**, 7012 (2002); A. B. Trofimov, J. Schirmer, D. M. P. Holland, A. W. Potts, R. Maripuu, and K. Siegbahn, J. Phys. B **35**, 5051 (2002); A. W. Potts, D. M. P. Holland, A. B. Trofimov, J. Schirmer, L. Karlsson, and K. Siegbahn, *ibid.* **36**, 3129 (2003); M. S. Deleuze, J. Phys. Chem. A **108**, 9244 (2004); D. M. P. Holland, I. Powis, L. Karlsson, A. B. Trofimov, J. Schirmer, and W. von Niessen, Chem. Phys. **297**, 55 (2004).
[24] J. Schirmer, A. B. Trofimov, and G. Stelter, J. Chem. Phys. **109**, 4734 (1998).
[25] H. Sekino and R. J. Bartlett, Int. J. Quantum Chem., Quantum Chem. Symp. **18**, 255 (1984); J. Geertsen, M. Rittby, and R. J. Bartlett, Chem. Phys. Lett. **164**, 57 (1989); J. F. Stanton and R. J. Bartlett, J. Chem. Phys. **98**, 7029 (1993); D. C. Comeau and R. J. Bartlett, Chem. Phys. Lett. **207**, 414 (1993).
[26] H. Monkhorst, Int. J. Quantum Chem., Quantum Chem. Symp. **11**, 421 (1977); E. Dalgaard and H. J. Monkhorst, Phys. Rev. A **28**, 1217 (1983); H. Koch, H. J. A. Jensen, P. Jørgensen, and T. Helgaker, J. Chem. Phys. **93**, 3345 (1990); H. Koch and P. Jørgensen, *ibid.* **93**, 3333 (1990); D. Mukherjee and P. Mukherjee, Chem. Phys. **39**, 325 (1979); S. Gosh, D. Mukherjee, and D. Bhattacheryya, Chem. Phys. **72**, 161 (1982).
[27] J. Schirmer, Phys. Rev. A **43**, 4647 (1991).
[28] F. Mertins and J. Schirmer, Phys. Rev. A **53**, 2140 (1996).
[29] A. B. Trofimov, G. Stelter, and J. Schirmer, J. Chem. Phys. **111**, 9982 (1999).
[30] A. B. Trofimov, G. Stelter, and J. Schirmer, J. Chem. Phys. **117**, 6402 (2002).
[31] H. Nakatsuji and K. Hirao, Chem. Phys. Lett. **47**, 569 (1977); J. Chem. Phys. **68**, 2053 (1978); H. Nakatsuji, Chem. Phys. Lett. **59**, 362 (1978); Chem. Phys. Lett. **67**, 329 (1979); Chem. Phys. Lett. **67**, 334 (1979).
[32] R. J. Bartlett and J. F. Stanton, Rev. Comput. Chem. **5**, 65 (1994); J. F. Stanton and J. Gauss, J. Chem. Phys. **101**, 8938 (1994); J. C. Saeh and J. F. Stanton, *ibid.* **111**, 8275 (1999); S. Hirata, M. Nooijen, and R. J. Bartlett, Chem. Phys. Lett. **328**, 459 (2000); A. D. Yau, S. A. Perera, and R. J. Bartlett, Mol. Phys. **100**, 835 (2002).
[33] M. Ehara and H. Nakatsuji, Chem. Phys. Lett. **282**, 347 (1998); M. Ehara, M. Ishida, and H. Nakatsuji, J. Chem. Phys. **114**, 8990 (2001); J. Chem. Phys. **117**, 3248 (2002).
[34] M. Musial, S. A. Kucharski, and R. J. Bartlett, J. Chem. Phys. **118**, 1128 (2003).
[35] D. Sinha, S. K. Mukhopadhyay, R. Chaudhuri, and D. Mukherjee, Chem. Phys. Lett. **154**, 544 (1989); D. Mukhopadhyay, S. K. Mukhopadhyay, R. Chaudhuri, and D. Mukherjee, Theor. Chim. Acta **80**, 483 (1991).
[36] M. D. Prasad, S. Pal, and D. Mukherjee, Phys. Rev. A **31**, 1287 (1985); D. Mukherjee and W. Kutzelnigg, in *Many-Body Methods in Quantum Chemistry*, edited by U. Kaldor (Springer, Berlin, 1989).
[37] M. Nooijen and J. G. Snijders, Int. J. Quantum Chem., Quantum Chem. Symp. **26**, 55 (1992).
[38] M. Nooijen and J. G. Snijders, Int. J. Quantum Chem. **47**, 3 (1993); Int. J. Quantum Chem. **48**, 15 (1993).
[39] M. Nooijen and J. G. Snijders, Int. J. Quantum Chem. **102**, 1681 (1995).
[40] C. W. Murray and E. R. Davidson, Chem. Phys. Lett. **190**, 231 (1992).
[41] J. Olsen, P. Jørgensen, H. Koch, A. Balkova, and R. J. Bartlett, J. Chem. Phys. **104**, 8007 (1996).
[42] C. W. Bauschlicher, Jr. and P. R. Taylor, J. Chem. Phys. **86**, 2844 (1987).
[43] C. W. Bauschlicher, Jr. and P. R. Taylor, J. Chem. Phys. **85**, 2779 (1986).
[44] D. M. P. Holland, D. A. Shaw, M. A. Hayes, L. G. Shpinkova, E. E. Rennie, L. Karlsson, P. Baltzer, and B. Wannberg, Chem. Phys. **219**, 91 (1997).
[45] N. Jonathan, A. Morris, M. Okuda, K. J. Ross, and D. J. Smith, Discuss. Faraday Soc. **54**, 48 (1972).
[46] C. E. Moore, *Atomic Energy Levels* (U.S. National Bureau of Standards, Washington, 1949), Vol. I; (U.S. National Bureau of Standards, Washington, 1952), Vol. II; (U.S. National Bureau of Standards, Washington, 1958), Vol. III.
[47] K. Kimura, S. Katsumata, Y. Achiba, T. Yamazaki, and S. Iwata, *Handbook of HeI Photoelectron Spectra of Fundamental Organic Molecules* (Halsted, New York, 1981), and references therein.
[48] W. L. Meerts, F. H. de Leeuw, and A. Dymanus, Chem. Phys. **22**, 319 (1977).
[49] R. C. Mockler and G. R. Bird, Phys. Rev. **98**, 1837 (1955).
[50] B. Fabricant, D. Krieger, and J. S. Muenter, J. Chem. Phys. **67**, 1576 (1977).
[51] T. R. Dyke and J. S. Muenter, J. Chem. Phys. **59**, 3125 (1973).
[52] M. Wickliffe and R. Rollefson, J. Chem. Phys. **70**, 1371 (1979).
[53] J. Schirmer and A. B. Trofimov, J. Chem. Phys. **120**, 11449 (2004).
[54] J. Schirmer and F. Mertins, Int. J. Quantum Chem. **58**, 329 (1996).
[55] J. Schirmer and A. Thiel, J. Chem. Phys. **115**, 10621 (2001).
[56] H. Koch, A. S. de Merás, T. Helgaker, and O. Christiansen, J. Chem. Phys. **104**, 4157 (1996).
[57] M. W. Schmidt, K. K. Baldridge, J. A. Boatz, S. T. Elbert, M. S. Gordon, J. H. Jensen, S. Koseki, M. Matsunaga, K. A. Nguyen, S. J. Su, T. L. Windus, M. Dupuis, and J. A. Montgomery, Comput. Chem. (Oxford) **14**, 1347 (1993).
[58] *MOLCAS* version 5.4, K. Andersson, M. Barysz, A. Bernhardsson, M. R. A. Blomberg, D. L. Cooper, M. P. Fülscher, C. de Graaf, B. A. Hess, G. Karlström, R. Lindh, P. -Å. Malmqvist, T. Nakajima, P. Neogrády, J. Olsen, B. O. Roos, B. Schimmelpfennig, M. Schütz, L. Seijo, L. Serrano-Andrés, P. E. M. Siegbahn, J. Stålring, T. Thorsteinsson, V. Veryazov, and P. -O. Widmark, Lund University, Sweden (2002).
[59] Thiel, MOLCAS/ADC interface.
[60] K. P. Huber and G. Herzberg, *Molecular Spectra and Molecular Structure. IV. Constants of diatomic molecules* (Van Nostrand Reinhold, New York, 1979).
[61] J. L. Duncan, Mol. Phys. **28**, 1177 (1974).
[62] K. Takagi and T. Oka, J. Phys. Soc. Jpn. **18**, 1174 (1963).
[63] R. L. Cook, F. C. De Lucia, and P. Helminger, J. Mol. Spectrosc. **53**, 62 (1974).
[64] T. H. Dunning, Jr., J. Chem. Phys. **90**, 1007 (1989); D. E. Woon and T. H. Dunning, Jr., *ibid.* **98**, 1358 (1993).
[65] V. R. Saunders and J. H. van Lenthe, Mol. Phys. **48**, 923 (1983).
[66] GAMESS-UK is a package of *ab initio* programs written by M. F. Guest, J. H. van Lenthe, J. Kendrick, and P. Sherwood, with contributions from R. D. Amos, R. J. Buenker, H. van Dam, M. Dupuis, N. C. Handy, I. H. Hillier, P. J. Knowles, V. Bonacic-Koutecky, W. von Niessen, R. J. Harrison, A. P. Rendell, V. R. Saunders, K. Schoffel, A. J. Stone, and D. Tozer.
[67] T. H. Dunning, Jr., J. Chem. Phys. **53**, 2823 (1970); T. H. Dunning, Jr. and P. J. Hay, in *Methods of Electronic Structure Theory*, edited by H. F. Schaefer III (Plenum, New York, 1977), Vol. 2.
[68] A. Thiel, Code for evaluation of $\Sigma(\infty)$ from MOLCAS CI one-electron density matrices.
[69] G. Angonoa, O. Walter, J. Schirmer, M. K. Scheller, and A. B. Trofimov, Dyson ADC(3) code.
[70] H. Hennig, J. Breidbach, and L. S. Cederbaum, J. Chem. Phys. **122**, 134104 (2005).
[71] J. Breidbach, nD-ADC(3) code; extension of Dyson ADC(3) code by F. Tarantelli *et al.*
[72] D. M. P. Holland, A. W. Potts, A. B. Trofimov *et al.*, Chem. Phys. **308**, 43 (2005).
[73] M. Pernpointner and A. B. Trofimov, J. Chem. Phys. **120**, 4098 (2004); M. Pernpointner, *ibid.* **121**, 8782 (2004).
[74] R. Santra and L. S. Cederbaum, Phys. Rep. **368**, 1 (2002).